References

BANSIGIR, K. G. & IYENGAR, K. S. (1958). *Proc. Phys. Soc. London*, **71**, 225.
BANSIGIR, K. G. & IYENGAR, K. S. (1961). *Acta Cryst.* **14**, 727.
DUBENSKII, K. K., KAPLYANSKII, A. A. & LOZOVSKAYA, N. G. (1967). *Sov. Phys. – Solid State* (USA), **8**, 1644.
IYENGAR, K. S. (1955). *Nature, Lond.* **176**, 1119.
LAIHO, R. & KORPELA, A. (1968). *Ann. Acad. Sci. Fenn.* A, **6**, 272.
MUELLER, H. (1935). *Phys. Rev.* **47**, 947.
MUELLER, H. (1938). *Z. Kristallogr.* A, **99**, 122.
NIKITENKO, V. I. & MARTYNENKO, G. P. (1965). *Sov. Phys. – Solid State* (USA), **7**, 494.
RAHMAN, A. & IYENGAR, K. S. (1967). *Phys. Letters*, A**25**, 478.
SPANGENBERG, K. & HAUSSÜHL, S. (1957). *Z. Kristallogr.* **109**, 422.
SRINIVASAN, R. (1959). *Z. Phys.* **155**, 281.
TELL, B., WORLOCK, J. M. & MARTIN, R. J. (1965). *Appl. Phys. Letters*, **6**, 123.

Acta Cryst. (1970). A**26**, 133

Absorption Coefficients for Al 111 Systematics: Theory and Comparison with Experiment

BY P. A. DOYLE

School of Physics, University of Melbourne, Parkville, Victoria 3052, *Australia*

(*Received* 7 *March* 1969)

Simple physical models are taken to calculate thermal and electronic contributions to absorption coefficients in Al. *N*-beam systematic calculations are interpreted by means of 2-beam theory, making possible a comparison with the experimental values of Watanabe. The mean absorption coefficient agrees to within 25 per cent. Spherical aberration and thermal diffuse scattering within the objective aperture are shown to explain the poorer agreement for the anomalous absorption coefficient. It is concluded that weak beams are significant in the measurement of absorption coefficients. Weak systematic beams are shown to have a significant effect on the positions of the thickness fringe maxima. A brief comparison of 2- and *N*-beam rocking curves is given.

Introduction

The theoretical interpretation of absorption coefficients in electron diffraction has been considered by several authors, but has been incomplete. Many-beam calculations including absorption have been reported for example by Howie & Whelan (1960) for Al and by Goodman & Lehmpfuhl (1967) for MgO. However, they compared experiment with arbitrary models for the absorbing potential V_g^i, such as $V_g^i \propto V_g^r$. On the other hand, Meyer (1966) compared absorption coefficients for Si calculated on physical models with experimental values, by mean of 2-beam theory. In the present paper, many-beam calculations are combined with absorption coefficients based on physical models of the inelastic processes for Al. The theoretical values can then be compared with those measured from elastic Bragg beams by Watanabe (1964, 1966), and the importance of weak beams studied. Detailed attention is paid to systematic errors in the experiments which tend to increase the apparent values of the mean absorption coefficient and particularly of the anomalous absorption coefficients.

Calculation of absorption coefficients for Al

The principal contributions to inelastic scattering in Al come from phonon, plasmon and single electron excitations. The absorption coefficients due to each of these processes are calculated in this section, using approximate theories to describe each process.

(*a*) *Thermal diffuse scattering*

Hall & Hirsh (1965) gave expressions for the mean and anomalous absorption coefficients due to thermal diffuse scattering, μ_0^{TDS} and μ_g^{TDS} respectively, using an Einstein model to describe the lattice vibrations. They found

$$\mu_0^{\mathrm{TDS}} = \frac{2\pi\lambda^2}{\Omega}\int f^2(\mathbf{s})\,[1-\exp(-2M_s)]s\,ds \qquad (1)$$

and

$$\mu_g^{\mathrm{TDS}} = \frac{\lambda^2}{\Omega}\iint f(\mathbf{s})f(\mathbf{s}-\mathbf{g})\,[\exp(-M_g) - \exp(-\{M_s+M_{s\text{-}g}\})]s\,ds\,d\varphi \qquad (2)$$

where the scattering vector $\mathbf{s}$ lies on the Ewald sphere, and $s = \dfrac{2\sin\theta}{\lambda}$ for a scattering angle 2θ. The usual Debye–Waller factor is $\exp(-M_s)$, and Ω is the unit-cell volume.

Equations (1) and (2) were derived by treating the incident wave as a Bloch wave, using 2-beam theory, and the thermal diffuse waves as plane. However, Pogany (1968) has shown that the same results for μ_0^{TDS}, and μ_g^{TDS} for all reflexions g, are obtained if the

elastic scattering is treated as N-beam dynamic. Also, Hall (1965) found that the use of a many-phonon Debye model gives absorption coefficients within a few per cent of those based on the Einstein model. Therefore, (1) and (2) were used to find the contribution to absorption from thermal scattering, using numerical integration, and the change of coordinates described by Hall & Hirsch.* The parametric fit given by Doyle & Turner (1968) was used to find $f(\mathbf{s})$ for $|\mathbf{s}|<4$, and the Rutherford scattering formula was used for $|\mathbf{s}|>4$. Values calculated for Al 111 systematics at 40 kV and 300°K are listed in Table 1.

Table 1. *Calculated absorption coefficients for* 111 *systematic reflexions of* Al *at* 40 kV

Units: $\times 10^{-3}$ Å^{-1}

g	μ^P	μ^{TDS}	μ^{SE}	μ^{total}
000	1·448	0·667	0·235	2·350
111		0·591	0·053	0·644
222		0·440	0·047	0·487
333		0·288	0·038	0·326
444		0·165	0·029	0·194
555		0·081	0·020	0·101
666		0·032	0·013	0·045
777		0·007	0·008	0·015
888		−0·003	0·004	0·001

(*b*) *Plasmon excitation*

Ferrell (1957) showed that the path length Λ for excitation of a plasmon of energy ΔE, by an incident electron of energy E, is given by

$$d\frac{1}{\Lambda}=\frac{d\Omega}{2\pi a_0}\left[\frac{\theta_E G^{-1}(2\theta)}{(2\theta)^2+\theta_E^2}\right]$$

Here, $d\Omega$ is an element of solid angle at an angle of scattering 2θ, a_0 is the Bohr radius, and $\theta_E=\Delta E/2E$. The factor $G^{-1}(2\theta)$ resulted from the time-dependent Hartree self-consistent field used, and did not appear in the simpler theory (Ferrell, 1956). Writing $x=2\theta/\theta_c$, the absorption coefficient μ_0^P is readily shown to be

$$\mu_0^P=\frac{1}{\Lambda}=\frac{\theta_E}{a_0}\int_0^1\frac{xG^{-1}(x)}{x^2+(\theta_E/\theta_c)^2}\,dx\,. \qquad (3)$$

Ferrell (1957) gave expressions for $G^{-1}(x)$ for x near 0 and 1, and interpolated graphically for intermediate values. This method has been used in the present work (Fig. 1). Again, he gave a cut-off angle θ_c in good agreement with the experimental value found by Watanabe (1956) for Al, for which it follows that

$$\theta_c=0{\cdot}74(E_0/E)^{1/2}$$

where E_0 is the Fermi energy.

By the use of these data for θ_c and G^{-1}, μ_0^P was found by evaluating (3) numerically. The contribution of surface plasmons, and their effect on the volume plasmons (Ritchie, 1957) are omitted. The value for Al at 40 kV appears in Table 1.

(*c*) *Single electron excitation*

Although more complex theories have been given (Whelan, 1965; Ohtsuki, 1967; Pogany, 1968), the single electron contribution will be small compared with those already considered for Al, so that we may follow the treatment of Heidenreich (1962) without introducing serious error. He divided the electronic contribution into two parts:

(i) Excitation of the Al^{3+} core, for which he took a point core model. The present approach differs from that of Heidenreich only in that a relativistic expression is used for the one-electron core cross-section per atom, φ_c, and the effect of thermal vibration is included *via*

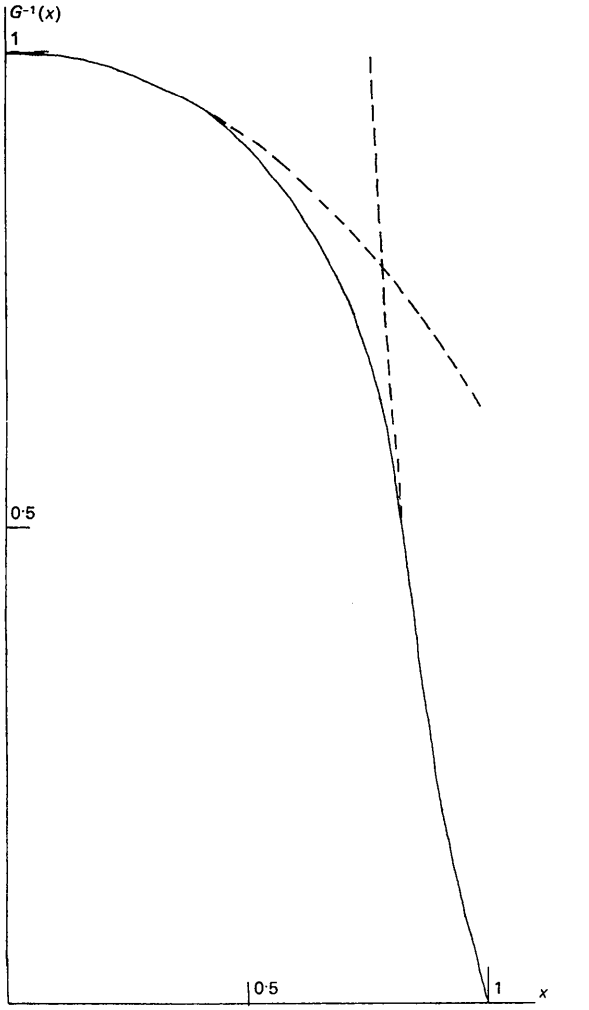

Fig. 1. The factor $G^{-1}(x)$, where $x=2\theta/\theta_c$, for the calculation of the plasmon contribution. The dashed lines are the asymptotic expressions given by Ferrell (1957).

* Note that the transformation between coordinate systems as stated by Hall & Hirsh is incorrect. Their expressions for $|\mathbf{s}|$ and $|\mathbf{s}-\mathbf{g}|$ should be interchanged, and in their notation, the parameter Y is given by

$$Y=\frac{\lambda g s'}{4}\cos\varphi'\sqrt{1/\lambda^2-s'^2/4}\,.$$

The numerical calculations reported by them appear to be based on this correct expression.

the Debye–Waller factor, as shown by Ohtsuki (1965). Then, it is easily shown, using the relativistic expression for φ_c given by Massey (1952), that

$$\mu_g^{SE} = \frac{h^2\sigma}{\pi m_0 e\lambda\Omega}\left(\frac{1}{137}\right)^2 \frac{B}{F}\ln\left(\frac{2F}{-\overline{\Delta\alpha}}\right)\exp(-M_g), \quad (4)$$

where

$$\sigma = \pi e/\lambda E$$
$$\gamma = m/m_0$$
$$\alpha = E/(m_0c^2\gamma)$$
$$-\overline{\Delta\alpha} = \langle\Delta E\rangle_{av}/(m_0c^2\gamma)$$
$$F = \gamma\alpha(\alpha+2)/(\alpha+1)^2 .$$

B is given by a sum over core electrons. Values of B and the average core excitation energy $\langle\Delta E\rangle_{av}$ are quoted by Heidenreich (1962) for Al^{3+}.

(ii) Scattering by the conduction electrons, taken to be free. The small angle scattering is represented by the plasmon excitation already considered. The large angle scattering is treated classically in the present work, using the Rutherford scattering cross-section

$$I(2\theta) = \left(\frac{e^2}{4\pi\varepsilon_0}\right)^2 \frac{\Delta}{16E^2\Omega\sin^4\theta} \quad (5)$$

where Δ is the number of conduction electrons per unit cell (3 for Al). The total cross-section is then given by

$$\varphi_F = 2\pi\int_{2\theta_{min}}^{\pi} I(2\theta)\sin(2\theta)d(2\theta) . \quad (6)$$

Classically, the response of an electron is small if the interaction time is long compared with the natural period of oscillation (see Massey (1952) for a discussion of this point). The minimum angle of scattering $2\theta_{min}$ is therefore taken to correspond to these two quantities being equal. Then, we find

$$2\theta_{min} = \left(\frac{\hbar^2e^2\gamma\Delta}{m_0\varepsilon_0\Omega E^2}\right)^{1/4} . \quad (7)$$

Ferrell (1957) showed that single electron excitation of conduction electrons does occur for all $2\theta \neq 0$, but that it will be small at low angles compared with plasmon excitation. The use of $2\theta_{min}$ above is therefore a further approximation.

Substituting (5) and (7) into (6), the single electron contribution to μ_0 from the free electrons is given by

$$\mu_0^{SEF} = \frac{h^2\sigma\varphi_F}{2\pi m\lambda\Omega} = \frac{\hbar e^2\sigma}{8\lambda E}\left(\frac{\Delta}{m_0\gamma^3\Omega\varepsilon_0{}^3}\right)^{1/2} . \quad (8)$$

Values of μ_0^{SE}, given by the sum of contributions from equations (4) and (8), and μ_0^{SE}, found from (4) with $g \neq 0$, are listed in Table 1.

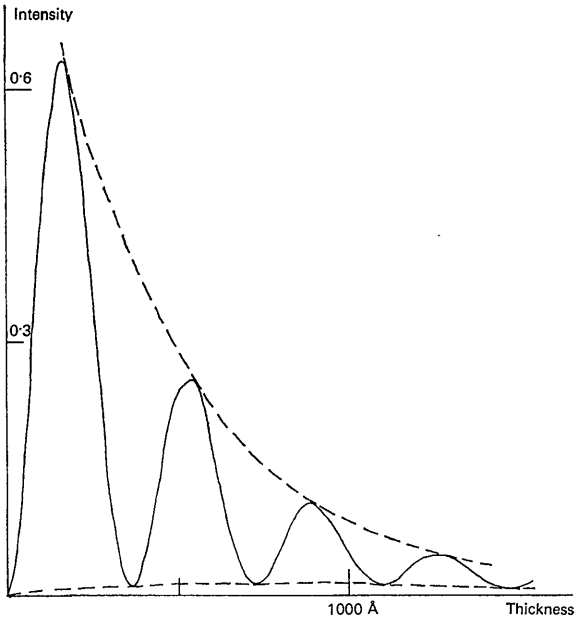

Fig. 2. N-beam thickness fringes for the 111 reflexion in Al at 40 kV, with that reflexion satisfied. The dashed curves represent the envelope of fringes. The intensity is normalized to a unit incident beam, therefore representing a probability. This procedure is used throughout the present paper.

Mean absorption coefficient

Absorption has been included in dynamical calculations by allowing the potential to become complex. The Fourier coefficients, v_g, for the potential of a centrosymmetrical crystal are then given by

$$v_g = v_g{}^r + iv_g{}^i$$

where $v_g{}^r$ are the usual coefficients of the thermally smeared out potential, and

$$v_g{}^i = \mu_g/2\sigma .$$

Many-beam calculations using the multi-slice program of Turner (1967) have been performed for Al 111 systematics, with absorbing potentials calculated as described above, and real potentials based on the atomic scattering factors of Doyle & Turner (1968). Single fundamental unit-cell layers were used, and 13 beams were included, from the $\overline{666}$ reflexion through to the 666 reflexion. Provided the Fourier coefficients out to the eighth order reflexion were included, for both real and absorbing potentials, when finding the projected potential of the unit cell, accurate numerical results were obtained. These theoretical thickness fringes are then interpreted using 2-beam theory, allowing the effect of weak beams on the measurement of absorption coefficients to be estimated, and making possible a comparison between the calculated and experimental values.

Fig. 2 shows thickness fringes for the 111 reflexion of Al at 40 kV, calculated with that reflexion exactly satisfied. The apparent value of μ_0 on the 2-beam approximation, ${}^{(2)}\mu_0$, is found using pairs of fringes, and the usual expression

$${}^{(2)}\mu_0 = 1/\xi_g \ln\left(\frac{2A_N}{2A_{N+1}}\right)$$

where ξ_g is the 2-beam extinction distance, and $2A_N$

is the difference between the top and bottom curves at the Nth peak height (see Fig.2, and Metherall (1967*a*) for a discussion). Table 2 shows values of ${}^{(2)}\mu_0$ calculated in this way from both dark and bright field images for Al at 40 kV. ξ_g was taken as 425 Å to correspond with the value used by Watanabe* (1964).

Table 2. *Values of mean absorption coefficient*

Theoretical $\mu_0 = 2{\cdot}35 \times 10^{-3}$ Å^{-1}

Units: $\times 10^{-3}$ Å^{-1}

Peaks used	Dark field ${}^{(2)}\mu_0$	Bright field ${}^{(2)}\mu_0$
1,2	2·24	2·25
2,3	2·13	2·09
3,4	2·22	2·30
4,5	2·23	2·67
5,6	2·22	1·71
${}^{(2)}\mu_0^{av}$	2·21	2·20
Experiment*	3·24, 3·20	2·98, 3·02

* Watanabe (1964) measured these values from elastic scattering only with a Möllenstedt-type energy filter.

The larger spread of values found from the bright field illustrates the greater deviation of this reflexion from the 2-beam approximation. The average values of ${}^{(2)}\mu_0$, ${}^{(2)}\mu_0^{av}$, are lower than the theoretical μ_0 because of the large value of ξ_g used. Again, ${}^{(2)}\mu_0^{av}$ is almost equal for bright and dark field, whereas the experimental value from the dark field is significantly higher. This may be caused by spherical aberration in the dark field experiment, which decreases contrast and therefore increases the apparent mean absorption. The bright field experimental value may then be more suitable for comparison with theory. Even this is subject to systematic errors tending to increase ${}^{(2)}\mu_0$, some of which will be considered in the following section. Comparing the values in bright field, it is concluded that the theoretical and experimental values of μ_0 agree to within 25 per cent. Also, it is apparent from Table 2 that the effect of weak beams is significant in determining μ_0, since ${}^{(2)}\mu_0^{av}$ is significantly different from μ_0.†

A further comparison can be made with the experiment of Watanabe (1966) for Al 111 at 75 kV. The theoretical μ_0 value is $1{\cdot}355 \times 10^{-3}$ Å^{-1}. The appropriate 2-beam interpretation of this gives ${}^{(2)}\mu_0^{av} = 1{\cdot}15 \times 10^{-3}$, which is to be compared with Watanabe's experimental value from dark field fringes, $1{\cdot}70 \times 10^{-3}$. The percentage difference is comparable with that for dark field at 40 kV in Table 2, so we may again expect the experimental value to be too high.

* The many-beam extinction distance for the 111 reflexion in this case is 367 Å. The difference is due about equally to Watanabe's use of the non-relativistic expression for ξ_g, and to the effect of weak beams. The different atomic models used for $v_g{}^r$ are relatively unimportant.

† If ξ_g is found using the relativistic 2-beam expression, ${}^2\mu_0^{av}$ is only slightly higher than μ_0. However, the 2 and many-beam extinction lengths are different by about 8 per cent in this case, so that the more accurate agreement of μ_0 values must be considered fortuitous.

Anomalous absorption coefficient

We have seen that the calculated value of μ_0 is within 25 per cent of the experimental value. On the other hand, Watanabe (1964) found $\mu_{111}/\mu_0 = 0{\cdot}4$ for Al at 40 kV, whereas the theoretical value from Table 1 is 0·27. This corresponds to about 50 per cent difference between theory and experiment for μ_{111}. In this section, a method for determining ${}^{(2)}\mu_{111}$, convenient for the present work, is established, then used together with approximate treatments of several systematic errors critical in the measurement of μ_{111} to explain the apparent discrepancy.

Anomalous absorption coefficients found from thickness fringes have generally been measured using the so-called 'centre curve' (Hashimoto, 1964). Since it is required to study deviations from the 2-beam prediction at different thicknesses, ${}^{(2)}\mu_{111}$ is found in the following way:

On 2-beam theory, it is apparent that the minima of the thickness fringes, I_N^{min}, lie on the curve

$$\exp(-\mu_0 z)\,[\cosh(\mu_{111} z) - 1]$$

when the 111 reflexion is exactly satisfied. Provided $z < 1/\mu_{111}$, it readily follows that

$${}^{(2)}\mu_{111} \simeq 2/\xi_g \exp\left(\frac{\mu_0 z_N}{2}\right)\left[\exp\left(\frac{\mu_0 \xi_g}{2}\right)\sqrt{I_{N+1}^{min}} - \sqrt{I_N^{min}}\right] \quad (9)$$

where the Nth minimum in the fringes occurs at z_N.

Using (9), values of ${}^{(2)}\mu_{111}$ can be calculated from pairs of minima in the fringes, and an average value ${}^{(2)}\mu_{111}^{av}$ found, when the 2-beam condition is satisfied. The value of μ_0 used is $2{\cdot}21 \times 10^{-3}$ Å^{-1}, since theoretical dark field fringes will be considered.

Several systematic errors in measuring μ_{111} will now be treated.

(*a*) *Thermal diffuse scattering under the objective aperture*

From the N-beam systematic calculations of thermal diffuse scattering (TDS) of Doyle (1969), it appears that TDS near the innermost Bragg reflexion does not generally differ from the kinematic value by more than about a factor of 2. Integrating dynamical TDS over the objective aperture is unduly complicated for the present purposes, and in any case multi-phonon processes were not included. Also, it is apparent from the calculations of Doyle that TDS is strongly affected by dynamical interactions other than 2-beam. This is because strong TDS occurs well out in the diffraction

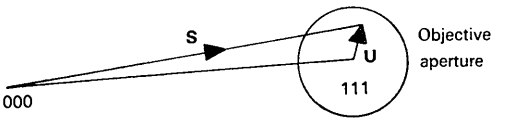

Fig. 3. The objective aperture in reciprocal space.

pattern, in contrast to the case of Bragg beams, for which most intensity is contained within 2 beams only. Since TDS will produce at best only weak fringe contrast, the 2-beam treatment (Natta, 1968) offers little advantage for the present work over an almost kinematic theory. The latter will therefore be used, together with a one-phonon Debye model.

Kinematically, the cross-section per unit crystal thickness for scattering by a phonon of wave vector $2\pi u$ lying on the Ewald sphere (Fig. 3) can be written

$$P'(\mathbf{s}) = \frac{s^2 f^2(\mathbf{s}) h}{2\varrho v \Omega^2 u} \coth \frac{hvu}{2KT} . \qquad (10)$$

Here, ϱ is the crystal density, v is the phonon velocity, assumed constant, K is Boltzmann's constant and T the absolute temperature. It has been assumed that the polarization vectors are orthogonal. Allowing TDS to follow a Poisson distribution, and remembering that intensity is lost from elastic and quasi-elastic waves at a rate approximately given by $\exp[-(\mu_0^P + \mu_0^{SE})z]$, TDS under the aperture may be written as

$$P_{111}^{TDS}(z) = Cz \exp(-\mu_0 z) \qquad (11)$$

where

$$C = \int_{\substack{\text{objective} \\ \text{aperture}}} P'(\mathbf{s}) d\mathbf{u} . \qquad (12)$$

Since the 2-beam condition is satisfied in the case of interest, a pole occurs in $P'(\mathbf{s})$ at the 111 position. This is overcome by noting after Takagi (1958) that dynamical thermal scattering is essentially forbidden for phonon wave vectors less than $2\pi/\xi_{111}$. Inserting (10) into (12) and integrating over the aperture, C is given approximately by

$$C = \frac{10^{30}}{47 \cdot 87^2} \cdot \frac{2\pi KT\lambda^2 v_{111}^2}{\varrho v^2 a^2} [\ln(\sinh y)]_{y_{min}}^{y_{max}} \text{ Å}^{-1} \qquad (13)$$

where

$$y_{min} = \frac{hv}{2KT} 1/\xi_{111}$$

and

$$y_{max} = \frac{hv}{2KT} \frac{0 \cdot 18}{a} .$$

The phonon velocity, v, was found from the Debye temperature as described for example by Hall (1965). The value of y_{max} corresponds to the objective aperture size used by Watanabe (1964). TDS under the aperture in his experiment is estimated, from (11) and (13), by

$$P_{111}^{TDS}(z) = 2 \cdot 79 \times 10^{-5} z \exp(-\mu_0 z) , \qquad (14)$$

with z in Å.

This expression should be adequate for the present purposes, but may tend to be low in general, since multi-phonon single- and multiple-scattering processes have been ignored.

(*b*) *Spherical aberration*

The effect of spherical aberration on ${}^{(2)}\mu_{111}$ measured from the dark field can be estimated from the values of μ_0 listed in Table 2. In dark field, the envelope of fringes is given by $\exp(-\mu_0^D z)$, and by $\exp(-\mu_0^B z)$ in bright field. Since the shapes of fringes at the peaks and valleys are similar, it seems reasonable to attribute half the decreased contrast in dark field to a decrease of the peak intensities, and half to an increase in the minimum intensities. Then, the additional intensity at the minima due to spherical aberration is given by

$$P_{111}^{SA}(z) \simeq \frac{\Delta\mu_0}{2} z \exp(-\mu_0^B z) \qquad (15)$$

where $\Delta\mu_0 = \mu_0^D - \mu_0^B = 0 \cdot 22 \times 10^{-3}$ Å^{-1} in Watanabe's experiment.

(*c*) *Convergence of incident beam*

Taking the angular spread of the incident beam as 5×10^{-4} radian corresponds to an increase in the apparent extinction distance by about 1 per cent, and in the values of I_N^{min} by about 10 per cent. The effect of this on ${}^{(2)}\mu_{111}$ is small compared with TDS or spherical aberration. However, more highly convergent incident beams, perhaps used to obtain greater intensity in an experiment, can become an important source of error, and should be avoided.

(*d*) *Additional effects*

Oxide layers formed on the surface, and the crystal support film, are ignored. Metherall (1967*b*) showed that the former tends to increase and sometimes decrease the apparent value of μ_0; it will presumably increase μ_{111} values, since I_N^{min} would be increased. It is supposed that the focusing of the image and the tilt setting of the crystal do not introduce any important errors. Any error in these would increase the measured values of both μ_0 and μ_{111}.

We are now in a position to study the effect of weak

Table 3. *Values of anomalous absorption coefficient from dark field*

Theoretical $\mu_{111} = 0 \cdot 644 \times 10^{-3}$ Å^{-1}
Units: $\times 10^{-3}$ Å^{-1}

Minima used	${}^{(2)}\mu_{111}^{BB}$	${}^{(2)}\mu_{111}^{BB+TDS}$	${}^{(2)}\mu_{111}^{BB+SA}$	${}^{(2)}\mu_{111}^{BB+TDS+SA}$	${}^{(2)}\mu_{111}^{TDS+SA}$
1,2	0·79	0·96	1·21	1·32	1·07
2,3	0·61	0·65	0·61	0·65	0·46
3,4	0·72	0·73	0·66	0·68	0·22
${}^{(2)}\mu_{111}^{av}$	0·71	0·78	0·83	0·88	0·58

BB, Bragg beams.
TDS, thermal scattering within objective aperture.
SA, background due to spherical aberration.

beams, TDS under the aperture and spherical aberration on the measurement of μ_{111}. Table 3 lists values calculated using (14) and (15) for the additional intensity at the positions z_N. The greater effect of the background scattering on ${}^{(2)}\mu_{111}$ values found from low thickness is due to both (14) and (15) being proportional to $z\exp(-\mu_0 z)$ whereas $I^{\min}$ is approximately proportional to $z^2\exp(-\mu_0 z)$, provided $z<1/\mu_{111}$. The background intensity is therefore relatively greater at low thickness.

When both important contributions to the background are included, ${}^{(2)}\mu_{111}^{\text{av}}$ is $0{\cdot}88\times10^{-3}$ Å^{-1}, compared with the theoretical value of $0{\cdot}644\times10^{-3}$ Å^{-1}. Remembering that the apparent value of μ_0 was decreased, the experimental ratio μ_{111}/μ_0 is predicted to be $0{\cdot}88\times10^{-3}/2{\cdot}21\times10^{-3}=0{\cdot}4$.

This is the value measured by Watanabe (1964). While the exact agreement should not be taken as significant, it is clear that the systematic errors involved in the experiment are of the correct order of magnitude to explain the apparently worse agreement for μ_{111} than for μ_0. If the values of $I_N^{\min}$ in (9) are taken as equal to the background intensity only, omitting the contributions due to the Bragg beams themselves, it is seen from Table 3 that ${}^{(2)}\mu_{111}^{\text{av}}$ is found to be $0{\cdot}6\times10^{-3}$ Å^{-1}. μ_g values lower than this could not be measured without reducing the background. Spherical aberration could be countered by the use of high resolution dark field techniques. TDS can be reduced by using low temperatures, remembering of course that the absorption coefficients themselves are dependent on temperature (as well as voltage and orientation). Reducing the aperture size gives some lowering in TDS, but (11) and (13) suggest that this approach does not offer such great improvement as might be anticipated.

The range of values of ${}^{(2)}\mu_{111}$, and the difference of their average from the theoretical value, show that it is desirable to account for weak beams in the determination of anomalous absorption coefficients. This conclusion was also reached by Goodman & Lempfuhl (1967), who used convergent beam methods together with an N-beam interpretation to find a value of μ_{200} for MgO significantly lower than those measured by earlier workers.

Rocking curves

Difficulty in fitting the centre and amplitude curves of thickness fringes for different tilts with the 2-beam theory has been reported for example by Uyeda & Nonoyama (1965) for MgO. While their experiment was performed without energy filtering, and will therefore be affected by inelastic scattering as well, it is instructive to compare the total elastically transmitted intensity, I^T, on 2- and N-beam theories for various crystal tilts. (The centre curve on 2-beam theory is just $I^T/2$.) Fig. 4 makes such a comparison for two thicknesses of Al 111 systematics at 40 kV, using the values of μ^{total} given in Table 1.

In general, 2-beam theory predicts the shape of the I^T curve well, though of course failing to produce the characteristic asymmetry around higher order reflexions, which becomes sharper with increasing thickness. The 2-beam theory slightly overestimates the elastic transmission for most tilts, and produces a small increase near zero tilt which is eliminated by the weak beams for this crystal. The agreement for the individual beams is not as good, as for example for the bright field rocking curve shown in Fig. 5.

Position of thickness fringe maxima

Including absorption in 2-beam theory, Goringe (1967) showed that the maxima in thickness fringes will be shifted from the position half-way between the minima, as is predicted when absorption is ignored. He expressed results in terms of a parameter δ, defined as the fraction of the extinction distance by which a particular maximum is shifted. A negative value of δ implies that the peak is shifted towards lower thickness. Table 4 gives values of δ on N-beam theory without absorption, and on N-beam and 2-beam theories, using

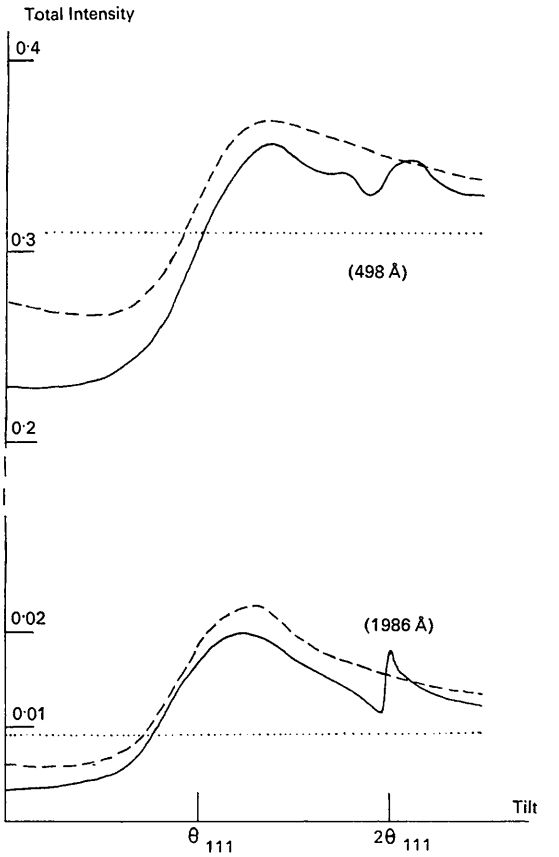

Fig. 4. Total elastically transmitted intensity as a function of tilt for two thicknesses of Al 111 systematics, using N-beam and 2-beam (dashed curve) theories. The dotted line is $\exp(-\mu_0 z)$, representing the transmission in the absence of the Borrmann effect.

the theoretical values of μ_0 and μ_g calculated at 75 kV as described above. The effects of weak beams and of absorption on the values of δ are seen to be of comparable importance. Thus while Goringe argued that the effect of absorption on δ would be significant in measuring absorption coefficients, it is apparent that weak beams must also be included.

Table 4. *Values of δ in dark field*

Al 111, 75 kV. The 111 reflexion is satisfied.

	N-beam		2-beam
Fringe number	No absorption	With absorption	With absorption
1	−0·008	−0·034	−0·035
2	−0·014	−0·063	−0·034
3	+0·024	−0·006	−0·033
4	−0·016	−0·031	−0·032

Discussion

It has been shown that the experimental and theoretical values of μ_0 for Al agree to within 25 per cent. The theoretical value is subject to the approximations discussed above. The apparently worse agreement for μ_{111} may partly be explained in terms of systematic errors inherent in the experiments.

The experimental determination of absorption coefficients should be interpreted using *N*-beam theory, taking care that crystals are tilted to truly systematic orientations. While two-dimensional dynamical calculations are certainly possible (Fisher, 1968; Turner, 1967), they involve lengthy computations due to the large number of beams required, and complicate the experiment unduly unless systematic orientations do not exist for a particular crystal. When dark field fringes are used, high resolution dark field techniques should be employed. For the measurement of anomalous absorption coefficients, thermal diffuse intensity under the objective aperture can be lowered by reducing the temperature and aperture size. The beam incident on the specimen must not deviate significantly from parallel illumination. The importance of oxide layers, and of filtering out inelastically scattered electrons, is already well known. Finally, 'nominal' microscope voltages do not seem to be sufficiently reliable. Therefore, it is necessary to measure the voltage at which an experiment is carried out before comparing the results with theoretical absorption coefficients.

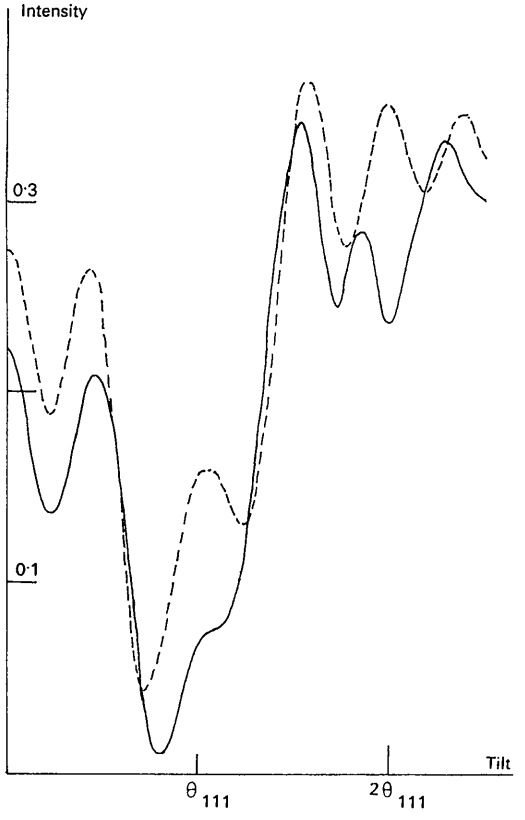

Fig. 5. Comparison of 2-beam (dashed curve) and *N*-beam rocking curves for the bright field of Al 111 systematics at 498 Å thickness.

The author is indebted to Dr P.S.Turner for permission to use his *N*-beam computer program, and to Professor J.M.Cowley for his critical reading of the manuscript. This work was partly supported by a grant from the Australian Research Grants Committee.

References

Doyle, P. A. (1969). *Acta Cryst.* A**25**, 569.
Doyle, P. A. & Turner, P. S. (1968). *Acta Cryst.* A**24**, 390.
Ferrell, R. A. (1956). *Phys. Rev.* **101**, 554.
Ferrell, R. A. (1957). *Phys. Rev.* **107**, 450.
Fisher, P. M. J. (1968). *Jap. J. Appl. Phys.* **7**, 191.
Goodman, P. & Lehmpfuhl, G. (1967). *Acta Cryst.* **22**, 14.
Goringe, M. J. (1967). *Phil. Mag.* **16**, 1111.
Hall, C. R. (1965). *Phil. Mag.* **12**, 815.
Hall, C. R. & Hirsch, P. B. (1965). *Proc. Roy. Soc.* A**286**, 158.
Hashimoto, H. (1964). *J. Appl. Phys.* **35**, 277.
Heidenreich, R. D. (1962). *J. Appl. Phys.* **33**, 2321.
Howie, A. & Whelan, M. J. (1960). *Proc. European Conf. Electron Microscopy*, Delft, p. 181.
Massey, H. S. W. (1952). *Advanc. Electronics*, **4**, 1.
Metherall, A. J. F. (1967*a*). *Phil. Mag.* **16**, 1103.
Metherall, A. J. F. (1967*b*). *Phil. Mag.* **16**, 763.
Meyer, G. (1966). *Phys. Letters*, **20**, 240.
Natta, M. (1968). *J. Phys. Radium*, **29**, 337.
Ohtsuki, Y. H. (1965). *J. Phys. Soc. Japan*, **20**, 1957.
Ohtsuki, Y. H. (1967). *Phys. Letters*, A**24**, 691.
Pogany, A. P. (1968). Ph.D. Thesis, Univ. of Melbourne.
Ritchie, R. H. (1957). *Phys. Rev.* **106**, 874.
Takagi, S. (1958). *J. Phys. Soc. Japan*, **13**, 287.
Turner, P. S. (1967). Ph.D. Thesis, Univ. of Melbourne.
Uyeda, R. & Nonoyama, M. (1965). *Jap. J. Appl. Phys.* **4**, 498.
Watanabe, H. (1956). *J. Phys. Soc. Japan*, **11**, 112.
Watanabe, H. (1964). *Jap. J. Appl. Phys.* **3**, 480.
Watanabe, H. (1966). *Electron Microscopy*, Vol. II. Ed. R.Uyeda. Tokyo: Maruzen.
Whelan, M. J. (1965). *J. Appl. Phys.* **36**, 2099.